J|A|C|S
ARTICLES
Published on Web 07/07/2006

Synthesis and Photophysical Properties of Borondipyrromethene Dyes Bearing Aryl Substituents at the Boron Center

Christine Goze,[†] Gilles Ulrich,[†] Laura J. Mallon,[‡] Ben D. Allen,[‡] Anthony Harriman,[‡] and Raymond Ziessel*,[†]

Contribution from the Laboratoire de Chimie Moléculaire, Centre National de la Recherche Scientifique (CNRS), École de Chimie, Polymères, Matériaux (ECPM), 25 rue Becquerel, 67087 Strasbourg Cedex 02, France, and Molecular Photonics Laboratory, School of Natural Sciences, Bedson Building, University of Newcastle, Newcastle upon Tyne, NE1 7RU, United Kingdom

Received April 7, 2006; E-mail: ziessel@chimie.u-strasbg.fr

Abstract: Several borondipyrromethene (Bodipy) dyes bearing an aryl nucleus linked directly to the boron center have been prepared under mild conditions. The choice of Grignard or lithio organo-metallic reagents allows the isolation of B(F)(aryl) or $B(aryl)_2$ derivatives; where aryl refers to phenyl, anisyl, naphthyl, or pyrenyl fragments. A single crystal, X-ray structure determination for the bis-anisyl compound shows that the sp^3 hybridized boron center remains pseudo-tetrahedral and that the B−C bond distances are 1.615 and 1.636 Å. All compounds are electrode active but replacement of the fluorine atoms by aryl fragments renders the Bodipy unit more easily oxidized by 100 mV in the B(F)(aryl) and 180 mV in the $B(aryl)_2$ compounds whereas reduction is made more difficult by a comparable amount. Strong fluorescence is observed from the Bodipy fluorophore present in each of the new dyes, with the radiative rate constant being independent of the nature of the aryl substituent. The fluorescence quantum yields are solvent dependent and, at least in some cases (aryl = anisyl or pyrenyl), nonradiative decay from the first-excited singlet state is strongly activated. There is no indication, however, for population of a charge-transfer state, in which the aryl substituent acts as donor and the Bodipy fragment functions as acceptor, that is strongly coupled to the ground state. Instead, it is conjectured that nonradiative decay involves a conformational change driven by the solvophobic effect. Thus, the rate of nonradiative decay in any given solvent increases with increasing surface accessibility (or molar volume) of the aryl substituent. Intramolecular energy transfer from pyrene or naphthalene residues to Bodipy is quantitative.

Introduction

Modern biotechnological and electronic applications require new fluorophores with predetermined properties, such as robustness, high fluorescence quantum yield, large Stokes' shift, optimized absorption profile and suitable anchoring groups, so as to meet the demands for more sensitive analytical protocols, sensors and light-emitting devices.[1,2] Among the many known classes of fluorescent dyes, the family of difluoro-boradiaza-indacenes (abbreviated herein as *F*-Bodipy), better known by the commercial name of BODIPY,[3] has received particular attention. The photophysical properties of this class of dyes are characterized by high fluorescence quantum yields, low rates of intersystem crossing, large molar absorption coefficients, excellent photostability, and an emission spectral profile that can be tuned over a wide range.[3,4,5] These properties have led to numerous applications in the field of biological labeling.[3,6] Furthermore, their electrochemical activity makes these dyes interesting candidates for use as dopants in light-emitting devices[7] and as components in electroactive films.

However, in common with most other organic fluorophores, *F*-Bodipy suffers from important inherent limitations. For example, such dyes possess small Stokes' shifts (around 600 cm^{-1}), that require the use of precision optical filters and specific excitation wavelengths for fluorescence microscopy and flow cytometry. A large Stokes' shift is of paramount importance in

[†] Centre National de la Recherche Scientifique (CNRS).
[‡] University of Newcastle.

(1) Valeur, B. In *Molecular Fluorescence: Principles and Applications*; Wiley-VCH: Weiheim, Germany, 2002.
(2) Lakowicz, J. R. *Probe Design and Chemical Sensing*; Lakowicz, J. R., Ed.; Topics in Fluorescence Spectroscopy Vol. 4; Plenum: New York 1994.
(3) Haugland, R. P. *The Handbook A guide to Fluorescent Probes and Labeling Technologies*, 10th ed.; Spence, M. T. Z., Ed.; Molecular Probes: Eugene, OR, 2005.
(4) Kang, H. C.; Haugland, R. P. U.S. Patent 5,451,663; Sep 19 1995.
(5) (a) Burghart, A.; Kim, H.; Welch, M. B.; Thoresen, L. H.; Reibenspies, J.; Burgess, K. *J. Org. Chem.* **1999**, *64*, 7813−7819. (b) Chen, J.; Burghart, A.; Derecskei-Kovacs, A.; Burgess, K. *J. Org. Chem.* **2000**, *65*, 2900−2906. (c) Turfan, B.; Akkaya, E. U. *Org. Lett.* **2002**, *4*, 2857−2859. (d) Coskun, A.; Akkaya, E. U. *J. Am. Chem. Soc.* **2005**, *127*, 10464−10465. (e) Qin, W.; Rohand, T.; Baruah, M.; Stefan, A.; Van der Auweraer, M.; Dehaen, W.; Boens, N. *Chem. Phys. Lett.* **2006**, *420*, 562−568.
(6) Martin, H., Rudolf, H., Vlastimil, F., Eds.; *Fluorescence Spectroscopy in Biology: Advanced Methods and their Applications to Membranes, Proteins, DNA, and Cells*; Springer-Verlag: Heidelberg, Germany, 2005.
(7) (a) Lai, R. Y.; Bard, A. J. *J. Phys. Chem. B* **2003**, *107*, 5036−5042. (b) Brom, J. M. Jr.; Langer, J. L. *J. Alloys Cmpds.* **2002**, *338*, 112−115. (c) Hepp, A.; Ulrich, G.; Schmechel, R.; von Seggern, H.; Ziessel R. *Synth. Met.* **2004**, *146*, 11−15.

10.1021/ja062405a CCC: $33.50

multicolor labeling (i.e., chromosome mapping) where sophisticated apparatus is used to simultaneously excite and analyze numerous fluorophores present in the system.[8] Several approaches are available by which to create an artificially large Stokes' shift. The most popular way involves the design of a tandem molecular device in which fluorescence resonance energy transfer occurs between discrete subunits; for example, the development of fluorescence energy-transfer cassettes based on modified oligo-deoxynucleotides[9] has resulted in greatly enhanced sensitivity for DNA recognition. In this way, an anthracene-based donor has been covalently linked to various *F*-Bodipy acceptors,[10] leading to efficient intramolecular energy transfer in a family of cassette dyes having a common excitation wavelength and a tunable emission range. Further examples of this approach have involved intramolecular energy transfer from an appended pyrene-based chromophore to *F*-Bodipy, with the aryl hydrocarbon being attached at the central pseudo-meso position.[11] Somewhat related systems have coupled fluorescent proteins possessing strong absorption profiles to other organic dyes, such as Alexa647.[3]

From a synthetic viewpoint, the multiple functionalization of *F*-Bodipy dyes is of particular interest but the scope is limited by the tedious pyrrole chemistry and by the condensation step that leads to the dipyrromethene intermediate. To circumvent the linear multistep syntheses needed for preparation of new Bodipy-based dyes[4,5] we recently introduced the concept of Cascatelle devices, in which a supplementary pendant arm enables bio-labeling of proteins.[12] Replacement of the fluorine atoms ubiquitous to *F*-Bodipy dyes with ethynyl-aryl moieties, thereby leading to *E*-Bodipy, is a further strategy for obtaining enlarged (virtual) Stokes' shifts.[12] Two examples of the replacement of the B−F units with B-phenyl fragments, and their basic physical properties, were described in a patent by Murase et al.[13] Aryl-Grignard reagents were found to be effective for fluorine replacement. Similar reactions using organo-metallic carbanions have been described with β-diketiminate boron complexes, leading to insertion of a tetrahedral boron center structurally related to difluoro-boradiazaindacene.[14] Trigonal boron salts have been converted to triaryl boron derivatives by way of organo-metallic species, mostly aryl-Grignard[15] or organo-lithium reagents,[16] and the resulting BR_3 compounds are stabilized with amino-donor groups. These synthetic procedures have been used to build dendritic scaffolds with extended π-conjugated systems including several boron centers[17] in order to obtain colorimetric fluoride ion sensors.[18] Here, we introduce a new family of fluorophores in which an aryl unit is connected directly to the boron center in place of the regular fluorine atoms on a boradiazaindacene scaffold (*C*-Bodipy). It is shown that these dyes are highly fluorescent in solution at ambient temperature but some interesting photophysical properties emerge as the size of the aryl substituent increases.

Scheme 1 [a]

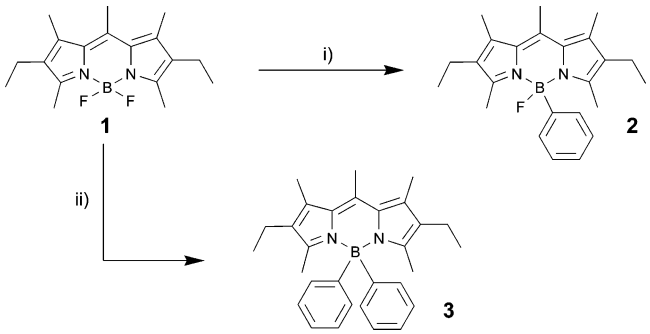

[a] Keys. (i) Phenylmagnesium bromide (1 equiv), diethyl ether, 1 h, 0 °C; (ii) Phenylmagnesium bromide (2 equiv), diethyl ether, 1 h, rt.

Scheme 2 [a]

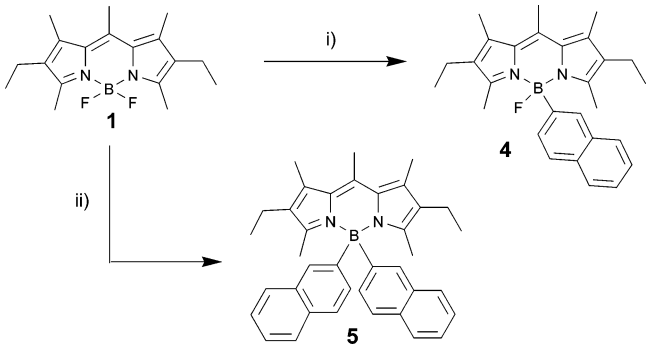

[a] Keys. (i) 2-Naphthylmagnesium bromide (1 equiv), diethyl ether, 2 h, 0 °C; (ii) 2-Naphthylmagnesium bromide (2 equiv), diethyl ether, 2 h, rt.

Results and Discussion

To validate the fluorine substitution process, an aryl-Grignard was reacted with the *F*-Bodipy **1** in anhydrous diethyl ether at room temperature (Scheme 1), following the general conditions described by Murase.[13] When arylmagnesium bromide is added at 0 °C, the major product is the monosubstituted derivative **2**, this being isolated in 40% yield. The disubstituted compound **3** cannot be observed by TLC, even with an excess of the Grignard reagent. Under these latter conditions, an intractable mixture of polar compounds is formed. However, the disubstituted derivative was obtained by adding the appropriate carbanion to a solution of the *F*-Bodipy at room temperature, giving rise to **3** in 25% yield (Scheme 1).

This procedure was subsequently applied to the synthesis of naphthalene-based analogues, using 2-naphthylmagnesium bromide, generated from 2-bromonaphthalene and magnesium turnings in diethyl ether. With this carbanion, the monosubstituted compound **4** was obtained in 30% yield by addition at 0 °C and the disubstituted compound **5** could be synthesized in 35% yield at 20 °C (Scheme 2). It was noted that additional red-colored, polar compounds were also obtained under these

(8) Ju, J.; Ruan, C.; Fuller, C. W.; Glazer, A. N.; Mathies, R. A. *Proc. Natl. Acad. Sci. U.S.A.* **1995**, *92*, 4347−4351.
(9) (a) Glazer, A. N.; Mathies, R. A. *Curr. Opin. Biotech.* **1997**, *8*, 94−102. (b) Berti, L.; Xie, J.; Medintz, I. L.; Glazer, A. N.; Mathies, R. A. *Anal. Biochem.* **2001**, *292*, 188−197.
(10) Wan, C.-W.; Burghart, A.; Chen, J.; Bergström, F.; Johanson, L. B.-A.; Wolford, M. F.; T. G. Kim, M. R. Topp, R. M. Hochstrasser, K. Burgess *Chem.−Eur. J.* **2003**, *9*, 4430−4441.
(11) Ziessel, R.; Goze, C.; Ulrich, G.; Césario, M.; Retailleau, P.; Harriman, A.; Rostron, J. P. *Chem.−Eur. J.* **2005**, *11*, 7366−7378.
(12) Ulrich, G.; Goze, C.; Guardigli, M.; Roda, A.; Ziessel, R. *Angew. Chem., Int. Ed.* **2005**, *44*, 3694−3698.
(13) Murase, S.; Tominaga, T.; Kohama, A. Eur. Patent EP 1253151a1, 25.04.2002.
(14) Qian, B.; Baek, S. W.; Smith, M. R. III *Polyhedron*, **1999**, *18*, 2405−2414.
(15) Brown, H. C.; Racherla, U. S. *J. Org. Chem.* **1986**, *51*, 427−432.
(16) Bayer M. J.; Pritzkow, H.; Siebert, W. *Eur. J. Inorg. Chem.* **2002**, 2069−2072.
(17) Yamaguchi, S.; Akiyama, S.; Tamao, K. *J. Am. Chem. Soc.* **2000**, *122*, 6335−6336.
(18) (a) Yamaguchi, S.; Akiyama, S.; Tamao, K. *J. Am. Chem. Soc.* **2001**, *123*, 11372−11375. (b) Kubo, Y.; Yamammoto, M.; Ikeda, M.; Takeuchi, M.; Shinkai, S.; Yamaguchi, S.; Tamao, K. *Angew. Chem., Int. Ed.* **2003**, *42*, 2036−2040.

Scheme 3 [a]

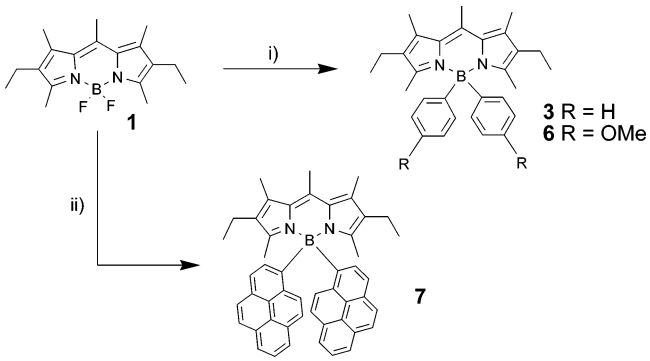

[a] Keys. (i) Phenyllithium (2 equiv) or 4-methoxyphenyllithium (2 equiv), diethyl ether, rt, 5 min, **3** (40%), **6** (35%); (ii) 1-pyrenyllithium (2 equiv), THF, rt, 5 min, 20%.

conditions but all attempts to isolate these latter materials were unsuccessful.

To compare the reactivity of the two organo-metallic carbanions used traditionally in the synthesis of arylboron derivatives, compound **3** was synthesized using phenylithium in diethyl ether. This reaction was carried out at various temperatures (−78, 0, 20 °C), and was much faster than that with the Grignard reagent. The reaction, however, has to be quenched rapidly to avoid formation of secondary polar products. Surprisingly, only formation of the disubstituted compound **3** was observed, even when 1 equiv of anion was used. This method was extended to other aromatic substituents, with the organo-lithium compound being generated at low temperature (−78 °C) by reaction of *n*-butylithium with an aryl bromide in THF. This latter solvent is used to increase the solubility of the starting compound. The aryllithium derivative is transferred to an *F*-Bodipy solution maintained at room temperature, and the reaction is quenched rapidly with water (5 min). The resultant products were stable and purified by column chromatography, followed by recrystallization. Compounds **6** and **7** were obtained in reasonable yields (20−35%), starting respectively from 4-methoxyphenyllithium and 1-pyrenyllithium (Scheme 3).

All new compounds were fully characterized by ^{1}H, ^{13}C, and ^{11}B NMR, mass spectroscopy and elemental analysis. In ^{1}H NMR spectra, typical peaks due to the Bodipy core can be observed; a characteristic feature being shielding of the singlet corresponding to the methyl group α to the nitrogen, this signal being shifted from 2.49 ppm for **1** to 2.16 ppm for **2**. Stronger shielding, induced by the phenyl ring, is observed for **3**, with a singlet appearing at 1.70 ppm. Similar behavior is observed for each of the other compounds, with the chemical shift of this methyl group moving from 2.39 ppm in the mononaphthyl derivative **4** to 1.73 ppm in the binaphthyl compound **5**. The strongest shielding was observed with the bis-pyrene derivative **7**, where the singlet appears at 1.32 ppm.

In ^{11}B NMR spectra, the triplet seen at 3.8 ppm can be attributed to coupling with the two equivalent fluorine atoms in **1**. This signal is replaced by a unique singlet for the other compounds, even for the mono-fluoro derivatives. The signal shifts downfield by ca. 2 ppm for the monosubstituted *C*-Bodipy whereas for the dipyrenyl compound the signal is shielded upfield 1.2 ppm with respect to the BF_2-starting material.

X-ray Crystallography. Single crystals were obtained for compounds **5** and **6** used to elucidate the X-ray molecular

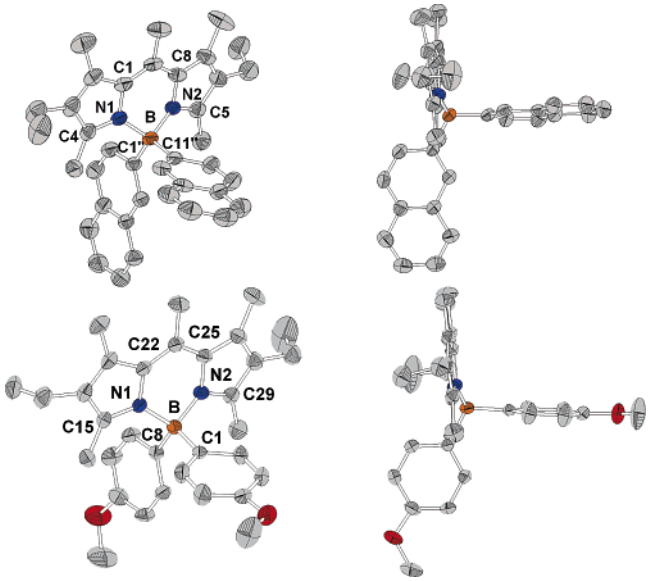

Figure 1. ORTEP views of compound **5** (Top) and **6** (bottom).

structure (Figure 1). Both structures are similar and only the structure of **6** and is discussed. The sp^3 hybridized boron center appears as a distorted tetrahedron with dihedral angles N1−B−N2 of 104.54° and C1−B−C2 of 114.96°. The diazaindacene unit is almost planar, with internal bond lengths slightly different to those of related *F*-bodipy analogues.[19] The boron atom is out of plane of the cyanine, being 0.50 Å from the mean plane; this deformation is not observed in *F*-Bodipy or *E*-Bodipy.[12] The average B−N bond length is 1.583 Å, this being slightly longer than that observed in *F*-bodipy (around 1.54 Å). The bond length in the diazaindacene core is similar to that found for *F*-bodipy derivatives,[19] with average bonds values for N1−C15/N2−C29 being 1.353(4) Å; these data tend to confirm the pronounced double-bond character. The C22−N1/C25N2 bond is longer, being 1.404 (5) Å. The B−C bonds in **6**, 1.615(4) for B−C1 and 1.636(4) for B−C2, are slightly longer than those found for somewhat similar 5-(2-pyridyl)pyrazolate diphenyl boron complexes.[20] Interestingly, in both structures the boron atom is located above the mean plane of the dipyrromethene residue by 0.50 Å for **6** and 0.57 Å for **5**, a situation which has never been observed in related *F*-Bodipy dyes where the boron center fits perfectly in the mean plane of the indacene core.[11,12]

Electrochemical Properties. An evaluation of the extent of electronic interactions between the various subunits in these new dyes was made by cyclic voltammetry in dichloromethane with tetra-*n*-butylammonium hexafluorophosphate as supporting electrolyte. The electrochemical data collected for the B-aryl molecules are gathered in Table 1. The prototypic starting material **1** displays a one-electron, reversible oxidation wave with a half-wave potential of +0.95 V vs SCE. There is a corresponding one-electron, reversible reduction wave with a half-wave potential of −1.43 V vs SCE. In comparison, compounds **2** and **3**, which lack one or both fluorine atoms respectively, are easier to oxidize, with half-wave potentials being lowered by 100 and 180 mV, respectively. Reduction is

(19) Shen, Z.; Röhr, H.; Rurack, K.; Uno, H.; Spieles, M.; Schulz, B.; Reck, G.; Ono, N. *Chem.—Eur. J.* **2004**, *10*, 4853−4871.
(20) Cheng, C.-C.; Yu, W.-S.; Chou, P.-T.; Peng, S.-M.; Lee, G.-H.; Wu, P.-C.; Song, Y.-W.; Chi, Y. *Chem. Commun.* **2003**, 2628−2629.

Table 1. Electrochemical Properties of the C−Bodipy Dyes and Reference Compound[a]

	$E_{1/2}$, V (ΔE, mV)			
cmpd	aryl$^{+\cdot}$/aryl	bodipy^{+}/bodipy	bodipy/bodipy$^{-\cdot}$	aryl/aryl$^{-\cdot}$
1		+0.95(70)	−1.43(60)	
2		+0.85(70)	−1.61(60)	
3		+0.77(60)	−1.79(70)	
4		+0.86(70)	−1.62(70)	
5	+1.60(irrev, $I_c/I_a \approx 0.1$)	+0.78(60)	−1.74(70)	
6	+1.64(irrev, $I_c/I_a \approx 0.1$)	+0.74(60)	−1.77(70)	
7	+1.48(irrev, $I_c/I_a \approx 0.2$)	+0.79(60)	−1.76(70)	−2.46(irrev)[b]

[a] Potentials determined by cyclic voltammetry in deoxygenated CH_2Cl_2 solution containing 0.1 M $TBAPF_6$, at a solute concentration of ca. 1 mM and at 20 °C. Potentials were standardized versus ferrocene (Fc) as internal reference and converted to SCE assuming $E_{1/2}$ (Fc/Fc^+) = +0.38 V (ΔE_p = 70 mV) vs SCE. Error in half-wave potentials is (±10 mV. Where the redox process is irreversible, the peak potential (E_{ap}) is quoted and the relative peak heights are given as I_c/I_a. All reversible redox steps result from one-electron transfer. [b] In 1,2-dichlorobenzene using a Hg hanging drop electrode. $I_c/I_a \approx 0$.

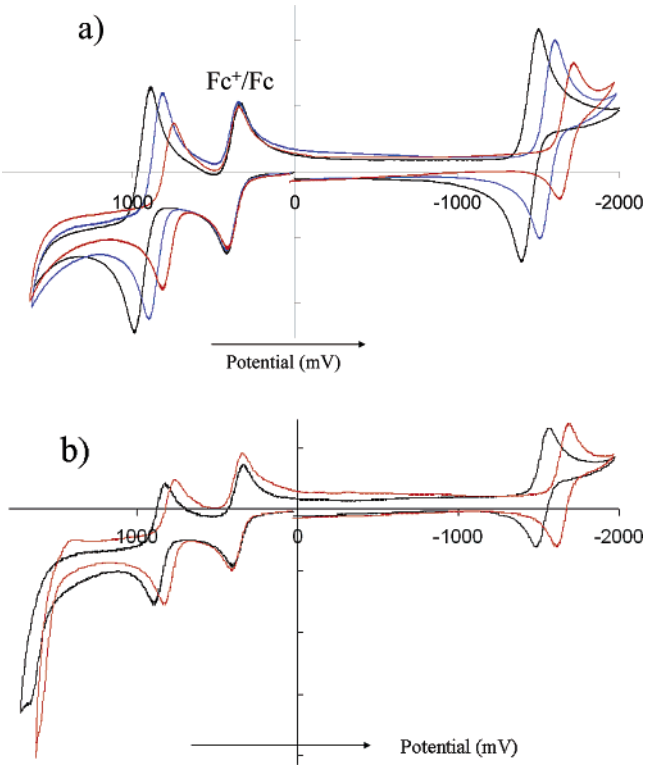

Figure 2. Cyclic voltammetry in CH_2Cl_2 at 20 °C using 0.1 M $^nBu_4PF_6$ as supporting electrolyte at a scan rate of 200 mV/s. (a) Compounds **1** (black), **2** (blue), and **3** (red). (b) Compounds **4** (black) and **5** (red). Ferrocene is used as internal standard (half-wave potential = 0.38V vs SCE).

more difficult, with the corresponding half-wave potentials being decreased by 180 and 360 mV, respectively, relative to **1** (Figure 2a). Both processes remain electrochemically reversible. There is no indication for oxidation to the Bodipy dication or reduction to the Bodipy dianion within the given electrochemical window, as observed previously for pyridine-linked B−F derivatives.[21] There is a small lowering (i.e., 30 mV) of the half-wave potential for one-electron oxidation on replacing the phenyl rings with anisole units, compound **6**.

On replacing the phenyl rings in compound **3** with naphthyl groups, in compound **5**, or pyrenyl units, in compound **7**, the various half-wave potentials remain essentially unaffected. It is apparent that the presence of the directly attached aryl moieties renders the indacene unit more easy to oxidize but more difficult to reduce. This observation can be explained in terms of increased electron density at the indacene core. It is also noticeable that in the anisyl, naphthyl and pyrenyl cases an additional, irreversible oxidation wave is present in the cyclic voltammograms. This latter wave can be assigned to one-electron oxidation of the aryl nucleus. As expected in light of previous observations[11] the pyrenyl residue is easier to oxidize than either the anisyl or naphthyl groups. For the pyrene compound **7**, an additional electrode process could be detected at about −2.5 V vs SCE in *ortho*-dichlorobenzene using a mercury hanging drop electrode.[11] This step is assigned to reduction of the pyrene unit.

It is interesting to note that the energy gap between LUMO and HOMO localized on the Bodipy dye is increased significantly for the B-aryl derivatives relative to the parent dye, **1**. Thus, the energy gap increases from 2.38 to 2.56 eV on replacing both fluorine atoms with phenyl rings. Replacing only a single fluorine atom results in an energy gap of 2.46 eV, midway between the disubstituted cases. The same behavior is seen for the corresponding naphthyl derivatives, where the energy gaps are 2.48 and 2.52 eV respectively for mono- and disubstitution. The nature of the aryl substituent has little real effect on this energy gap, being 2.55 eV for pyrenyl and 2.51 eV for anisyl substituents. The overall difference, however, between **1** and **3** is surprisingly pronounced.

Optical Properties. Spectroscopic data relevant to the present discussion are collected in Table 2. In solution, the absorption spectra of all compounds show a strong $S_0 \rightarrow S_1$ ($\pi-\pi^*$) transition with a clear maximum (λ_{MAX}) between 510 and 525 nm. In most cases, the molar absorption coefficient at the peak (ϵ_{MAX}) has a value of about 75 000 M^{-1} cm^{-1}. This transition is unambiguously assigned[5,22] to the Bodipy chromophore and it is noteworthy that, except for **7**, the B-aryl dyes show somewhat larger ϵ_{MAX} values than the parent dye **1**. This is not the case for the pyrene-based dye **7** where the lowest-energy absorption band is noticeably broader and weaker. In all cases, a broad absorption band, that can be assigned to the $S_0 \rightarrow S_2$ ($\pi-\pi^*$) transition[23] of the boradiazaindacene unit, is located between 370 and 410 nm (Figure 3). Additional $\pi-\pi^*$ transitions are found around 250 and 280 nm, respectively, for the phenyl and the naphthyl residues, although these overlap higher-energy bands due to the dye. For the pyrenyl fragments, $\pi-\pi^*$ transitions can be seen across much of the near-UV region with two clear sets of bands around 320−370 nm and 230−310 nm (Figure 3). The lowest-energy absorption transition association with the pyrene fragment is seen as a weak, sharp band at about 375 nm in dichloromethane. No evidence was obtained for self-association of these compounds in dichloromethane solution, at least at concentrations below 2 mM.

An interesting, if fortuitous, feature of the optical absorption spectrum recorded for **1** is that the energy of the absorption maximum (λ_{MAX} = 2.40 eV) is in excellent agreement with the energy gap between LUMO and HOMO (Δ = 2.38 eV) obtained from cyclic voltammetry. It is also clear that whereas λ_{MAX} for **1** is essentially insensitive to changes in solvent polarity, those

(21) Ulrich, G.; Ziessel, R. *J. Org. Chem.* **2004**, *69*, 2070−2083.

(22) Kollmannsberger, M.; Rurack, K.; Resch-Genger, U.; Daub, J. *J. Phys. Chem. A* **1998**, *102*, 10211−10220.

(23) Karolin, J.; Johansson, L. B.-A.; Strandberg, L.; Ny, T. *J. Am. Chem. Soc.* **1994**, *116*, 7801−7806.

Table 2. Spectroscopic Data for the Various Dyes in Solution at 298 K

cmpd	λ_{MAX}[a] (nm)	ϵ_{MAX}[a] ($M^{-1}cm^{-1}$)	λ_{FLU}[a] (nm)	Φ_{FLU}[a]	τ_{FLU}[a] (ns)	k_{RAD}[b] (10^8 s^{-1})	λ_{FLU} (nm)[c]	Φ_{FLU}[c]	τ_{FLU}[c] (ns)	Φ_{FLU}[d]	τ_{FLU}[d] (ns)
1	517	64 500	538	0.83	6.2	1.35	536	0.90	6.7	0.88	6.6
2	524	75 200	543	0.90	6.4	1.40	-	-	-	-	-
3	513	73 300	548	0.91	6.1	1.50	539	0.77	5.0	0.76	5.0
4	513	77 300	543	0.92	6.1	1.50	-	-	-	-	-
5	516	74 500	552	0.80	5.7	1.40	541	0.65	4.9	0.60	5.0
6	513	77 400	546	0.78	6.0	1.30	540	0.64	4.7	0.57	4.8
7	526	46 000	562	0.19	2.0	0.95	558	0.12	1.7	0.14	1.6

[a] Determined in deoxygenated dichloromethane solution. [b] Calculated from the Strickler−Berg expression. [c] Ethanol solution. [d] Acetonitrile solution.

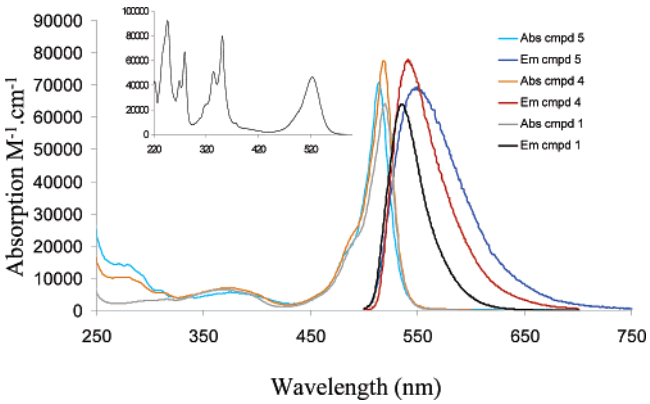

Figure 3. Absorption spectra, emission spectra (arbitrary units) for compounds **1**, **4**, and **5**. Absorption of **7** is shown as an inset. All spectra were measured in CH_2Cl_2 at room temperature.

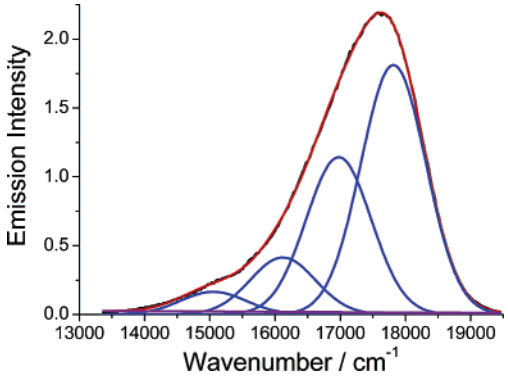

Figure 4. Fluorescence spectrum (black curve) observed for **7** in ethanol solution. The blue curves represent the deconvoluted Gaussian components whose maxima are separated by the low-frequency vibrational mode $h\omega_L$. The sum of the Gaussian bands, red curve, is compared to the total spectrum.

for the B-aryl derivatives tend to undergo a small red shift with increasing polarizability of the solvent. For example, λ_{MAX} for **6** is found at 516, 513, 512, 512, and 509 nm, respectively, in cyclohexane, dichloromethane, ethanol, dimethyl sulfoxide, and acetonitrile. A similar observation has been made for certain 3,5-disubstituted F-bodipy dyes.[5e]

The parent dye **1** fluoresces with high efficiency in solution at ambient temperature. The emission maximum (λ_{FLU}) is located at 538 nm in dichloromethane and is insensitive to changes in solvent polarity; for example, λ_{FLU} shifts to 536 nm in acetonitrile solution. The fluorescence quantum yield (ϕ_{FLU}) in deoxygenated dichloromethane is 0.83, where the fluorescence lifetime (τ_{FLU}) is 6.2 ns. Again, changes in solvent polarity have minimal effect on these values (Table 2). The corrected fluorescence excitation spectrum agrees well with the absorption spectrum over the visible and near-UV regions and photons absorbed by the S_2 state are transferred quantitatively to S_1. The Stokes' shift is only 650 cm^{-1} in dichloromethane and is increased to 700 cm^{-1} in acetonitrile. The fluorescence decay profiles were strictly monoexponential in all solvents and the derived τ_{FLU} is independent of excitation or monitoring wavelength. The radiative rate constant calculated from the Strickler−Berg expression[24] ($k_{RAD} = 1.30 \times 10^8$ s^{-1}) is in excellent agreement with that estimated directly by experiment ($k_{RAD} = \phi_{FLU}/\tau_{FLU} = 1.35 \times 10^8$ s^{-1}). All available indicators point to minimal disruption of the geometry on excitation to the singlet manifold. It is also clear that nonradiative deactivation of the excited singlet state competes poorly with the radiative process.

Fluorescence is readily observed from the various B-aryl dyes following excitation into the first-excited singlet state in dichloromethane solution (Table 2). In each case, λ_{FLU} is red shifted with respect to **1** (Figure 4) but remains independent of excitation wavelength. Relative to **1**, the Stokes' shift is also larger, having a value of 1230 cm^{-1} for **7**, and sensitive to the size of the aryl substituent. With the exception of **7**, ϕ_{FLU} and τ_{FLU} measured for the new compounds in deoxygenated dichloromethane remain comparable to those recorded for **1**. In each case, fluorescence is clearly characteristic of the Bodipy fluorophore[5,22,23] and decay kinetics are monoexponential. For these dyes, k_{RAD} is found to be $1.3 \pm 0.2 \times 10^8$ s^{-1} in dichloromethane. There is, however, a modest decrease in both ϕ_{FLU} and τ_{FLU} in ethanol (Table 2), where the Stokes' shifts are decreased by ca. 20%. Similar values are found in acetonitrile but k_{RAD} remains solvent independent.[25] It is clear that there is an increase in the rate of nonradiative decay for the B-aryl compounds in these latter solvents, even for the phenyl-based dyes where intramolecular charge-transfer is most unlikely.

The disubstituted pyrene-based dye **7** exhibits a relatively low ϵ_{MAX} in the region where Bodipy absorbs and both ϕ_{LUM} and τ_{LUM} are decreased relative to the other B-aryl dyes (Table 2). The absorption profile of the pyrene component is red shifted and broadened with respect to pure pyrene[26] and the S_1-S_0 fluorescence spectrum observed for **7** is the most red shifted of the B-aryl dyes studied. Both ϕ_{LUM} and τ_{LUM} decrease in ethanol and acetonitrile, where the Stokes' shift remains at ca. 1200 cm^{-1}. For **7**, the radiative rate constant is about 9×10^7 s^{-1} in all solvents; the decrease relative to the other B-aryl dyes reflecting the drop in oscillator strength.[27] It is clear that, in all solvents, nonradiative decay plays an important role for this system. The same fluorescence spectral profile is observed

(24) Strickler, S. J.; Berg, R. A. *J. Chem. Phys.* **1962**, *37*, 814−817.

(25) (a) In fact, the small variation in k_{RAD} found in different solvents can be well explained in terms of changes in refractive index. (b) Meech, S. R.; Phillips, D. *J. Photochem.* **1983**, *23*, 193−217.

(26) Birks, J. B. *Photophysics of Aromatic Molecules*; Wiley-Interscience: New York, 1970.

(27) From the Strickler−Berg expression, k_{RAD} for the pyrene-based dye **7** is calculated to be 9×10^7 s^{-1} in dichloromethane solution.

Table 3. Derived Rate Constants for Nonradiative Decay of the First-Excited Singlet State of the Various Dyes in Different Solvents

cmpd	$h\omega_L$ (cm^{-1})	V_{MOL} ($cm^3\ mol^{-1}$)	k_{NR}/CH_2Cl_2 ($10^7\ s^{-1}$)	k_{NR}/C_2H_5OH ($10^7\ s^{-1}$)	k_{NR}/CH_3CN ($10^7\ s^{-1}$)
3	1060	263.5	1.5	4.6	4.8
5	950	409.5	3.5	7.1	9.0
6	950	337.5	3.7	7.7	8.0
7	1010	619.5	37.5	51.8	56.2

following excitation into the pyrene unit. Furthermore, the corrected excitation spectrum matches with the absorption spectrum over the range 260 to 530 nm in all solvents studied. Thus, photons collected by the pyrene unit are transferred quantitatively to the Bodipy chromophore. The same is true for the naphthyl derivative **5**.

Detailed studies carried out with the anisyl derivative **6** showed that the Stokes' shift does not vary systematically with solvent polarity and, in particular, does not follow Lippert−Mataga behavior.[28] This suggests that there is not a large difference in dipole moment between ground and excited states. The same situation was found for **7**. Deconvolution[29] of the emission spectral profile (Figure 4) leads to the conclusion that nonradiative decay of the lowest-energy singlet excited state is coupled to a low-frequency vibrational mode ($h\omega_L$) of ca. $990 \pm 70\ cm^{-1}$ (Table 3), although the same analysis carried out for **1** showed a vibrational mode of ca. $650\ cm^{-1}$. There was no systematic effect of solvent polarity on the size of the coupled vibrational mode,[30] whereas similar analysis applied to the absorption spectral profiles for the S_0-S_1 transition gave comparable but consistently smaller $h\omega_L$ values.[31] Furthermore, the reorganization energies[32] (λ) accompanying formation of the S_1 state are larger for the B-aryl dyes than for the parent. Indeed, λ for the phenyl ($400\ cm^{-1}$), anisyl ($500\ cm^{-1}$) and naphthyl ($520\ cm^{-1}$) substituted Bodipy dyes significantly exceed that for **1** ($280\ cm^{-1}$) under identical conditions. The reorganization energy ($\lambda = 630\ cm^{-1}$) is somewhat larger for **7** than for the other dyes.

The fluorescence lifetime recorded for **1** in ethanol solution was found to be insensitive to changes in temperature over the range 100−300 K.[33] This was not the case for **6** where there is clear evidence for the onset of an activated decay route at higher temperature (Figure 5). Thus, in a frozen ethanol glass, τ_{FLU} remains constant at 10.2 ns, which is remarkably close to the radiative lifetime calculated under these conditions. Clearly, nonradiative decay is unimportant in the glassy matrix. On melting the glass, τ_{FLU} decreases to ca. 7 ns but remains

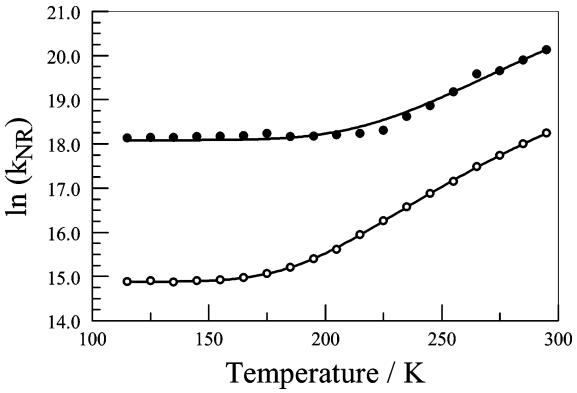

Figure 5. Effect of temperature on the rate constants for nonradiative decay as measured for **6** (○) and **7** (●) in ethanol. The solid line drawn through each set of data points is a nonlinear, least-squares fit to eq 1 with the parameters given in the text.

reasonably independent of temperature until around 230 K. Above this temperature, τ_{FLU} decreases smoothly with increasing temperature. Expressing the kinetic data obtained in fluid solution in the form of eq 1, where k_{NR} is the rate constant for nonradiative decay of the excited state, allows estimation of the activation energy for the activated decay route as being 17.7 kJ mol^{-1}. The derived activated preexponential factor (k_{ACT}) has a value of $1.1 \times 10^{11}\ s^{-1}$ while the activationless rate constant (k_{IND}) describing nonradiative decay at low temperature is calculated to be $2.9 \times 10^6\ s^{-1}$. The same behavior is found for **7** (Figure 5), where the activation energy is 19.4 kJ mol^{-1}. For this latter system, $k_{IND} = 7.1 \times 10^7\ s^{-1}$, whereas k_{ACT} has a value of $1.3 \times 10^{12}\ s^{-1}$. Nonradiative decay is much more pronounced for the bulkier pyrene substituent.

$$k_{NR} = \frac{(1 - \phi_{FLU})}{\tau_{FLU}} = k_{IND} + k_{ACT}e^{-(E_A/RT)} \qquad (1)$$

The additional nonradiative decay process characterized by k_{ACT} is solvent dependent and does not result in enhanced triplet state formation,[34] which remains extremely inefficient under all conditions. A possible explanation for the temperature effect could involve population of a high-lying, charge-transfer state (CTS) in which the aryl substituent acts as donor and the Bodipy residue functions as acceptor. The cyclic voltammetry results indicate irreversible oxidation of the anisole unit at about 1.64 V vs SCE but this value can be lowered to about 1.5 V vs SCE by allowing for electrostatic effects.[35] This would place the energy of any such CTS at about 3.1 eV in ethanol solution, but this is still 0.7 eV above the π,π^* excited singlet state associated with the Bodipy unit. Population of the CTS via a thermal process from S_1, therefore, is inconsistent with the observed activation energy. A similar conclusion is reached for **7**, although the energy of the CTS ($E_{CTS} \approx 2.9$ eV) is projected to be closer to that of the S_1 state ($E_S = 2.37$ eV). The

(28) (a) Lippert, E. *Z. Naturforsch. Teil A* **1955**, *10*, 541−545. (b) Mataga, N.; Kaifu, Y.; Koizumi, M. *Bull. Chem. Soc. Jpn.* **1956**, *29*, 465−470.
(29) (a) Smedarchina, Z.; Fernandez-Ramos, A.; Siebrand, W. *J. Comput. Chem.* **2001**, *22*, 787. (b) Chang, R.; Hsu, J. H.; Fann, W. S.; Liang, K. K.; Chang, C. H.; Hayashi, M.; Yu, J.; Lin, S. H.; Chang, E. C.; Chuang, K. R.; Chen, S. A. *Chem. Phys. Lett.* **2000**, *317*, 142−152.
(30) For example, for **6** $h\omega_L$ was determined from emission spectral profiles to be 923, 980, 948, 925, and 976 cm^{-1}, respectively, in dichloromethane, dimethyl sulfoxide, ethanol, hexane, and acetonitrile.
(31) For example, for **6** $h\omega_L$ was determined from absorption spectral profiles to be 871, 809, 911, 820, and 858 cm^{-1}, respectively, in dichloromethane, dimethyl sulfoxide, ethanol, hexane, and acetonitrile. Closely comparable values were obtained by analysis of the corrected excitation spectra.
(32) The total reorganization energy (λ) was calculated from the fluorescence spectrum by examining the temperature dependence for the half-width of the low-frequency vibrational modes and correcting for instrumental broadening.
(33) Harriman, A.; Rostron, J. P.; Cesario, M.; Ulrich, G.; Ziessel, R. *J. Phys. Chem. A* **2006**, ASAP.
(34) The triplet excited state was hardly detectable by laser flash photolysis studies carried out in deoxygenated solution following excitation with a 4-ns pulse. Recovery of the ground state, measured by following the bleaching signal at the absorption maximum, was essentially complete within the laser pulse. Low-temperature phosphorescence in an ethanol glass could not be detected, in any case.
(35) The electrostatic correction term was estimated by considering point charges separated by the distance between the midpoints of the aryl substituent and Bodipy framework. The distances were obtained from energy-minimized structures computed at the AM1 level. It was assumed that the point charges were embedded in a continuum solvent of known dielectric constant. It is recognized that such calculations are necessarily crude.

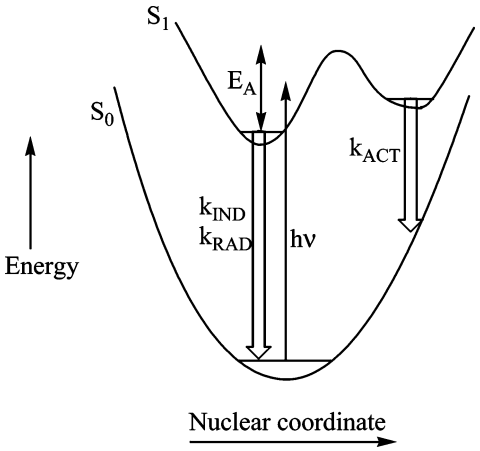

Figure 6. Simplified potential energy level diagram summarizing the proposed conformational change available to the excited singlet state. Excitation of the ground-state system produces a metastable geometry, after thermal equilibration, that undergoes fluorescence and activationless nonradiative decay. A more distorted geometry can be accessed by passage over a barrier, denoted by E_A. This "dark" state decays rapidly to re-form the ground state.

impression, therefore, is that charge-transfer effects are not responsible for the enhanced rates of nonradiative decay seen with these B-aryl dyes.

The rate constants for nonradiative decay at room temperature ($k_{NR} = (1 - \phi_{FLU})/\tau_{FLU}$) increase with increasing size of the aryl substituent and also depend on the nature of the solvent (Table S1).[5e] This finding can be used to suggest that k_{NR} is in some way connected to a steric effect. There is a crude correlation between k_{NR} and the molar volume (V_{MOL})[36] of the aryl substituent but this does not take into account the noted solvent effects. A more reasonable way to examine the data involves consideration of the solvent accessible surface area of the substituent and the solvophobicity of the aryl group. Thus, following an earlier study of somewhat related Bodipy-based dyes,[37] it is considered that the ground state conformation has a global minimum corresponding to a geometry related to the X-ray structure. Excitation into the excited singlet state manifold gives rise to a relaxed geometry that is not too dissimilar to that of the ground state (Figure 6). This relaxed geometry is responsible for the fluorescence observed in fluid solution. The excited state surface, however, is considered to possess several minima and, in competition to fluorescence, an activated geometry change is possible. Passage over a modest barrier, characterized experimentally by E_A in eq 1, provides access to a distorted geometry that has no ground-state counterpart (Figure 6). Nonradiative deactivation from this new geometry is fast because of the decreased energy gap and an increased Franck−Condon overlap factor.[38]

It is interesting to note that fluorescence from **7** is restored in the solid state at ambient temperature. Thus, τ_{FLU} is 5.9 ns when the sample is dispersed in a sucrose octa-acetate glass at 25 °C. Conformational changes are less likely to occur in the glass. In this medium, the fluorescence quantum yield was found to be essentially independent of temperature over the range 295 to 80 K. This finding is consistent with geometry changes playing a major role in promoting nonradiative decay for the dyes bearing large aryl substituents in fluid solution. It should, however, be noted that earlier work[5e,39] has also reported that for certain F-bodipy dyes k_{NR} increases with increasing polarity of the solvent. In most cases, this polarity effect can be traced to intramolecular charge-transfer effects associated with an aryl donor substituted at the meso position. Charge-transfer interactions are less likely in our systems, although such effects might make a minor contribution toward the observed k_{NR} values found in polar solvents.

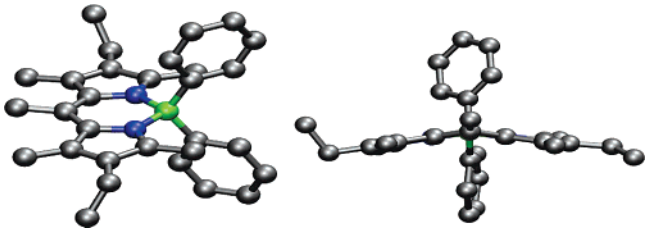

Figure 7. (a) Left-hand panel shows the computed geometry for the ground state of **3**. (b) Right-hand panel shows the computed lowest-energy geometry for the corresponding first-excited singlet state of **3**.

At present, the nature of the proposed conformational change is unknown, but it might involve concerted distortion of the indacene backbone, resulting in a shift from planar to bent geometries. Thus, the computed geometry of each of the new derivatives was found to be pseudotetrahedral around the boron center but with the indacene fragment being strictly planar (Figure 7a). The computed excited-state geometries show some measure of geometric distortion in the planarity of the indacene unit (Figure 7b).[40] The magnitude of this buckling effect increases with increasing size of the aryl substituent, corresponding to a distortion of about 22° for the pyrene-derivative **7**. The computed excitation energy for **3** ($\Delta = 2.54$ eV) is in excellent agreement with the HOMO−LUMO energy gap ($\Delta = 2.56$ eV) obtained by cyclic voltammetry, For none of the compounds, however, was the structural distortion accompanying excitation sufficient to account for the enhanced rates of nonradiative decay found in polar solvents. As such, we conclude that the driving force for conformational change is provided, in part, by the solvophobic effect. Here, the substituent seeks to minimize surface exposure to polar solvents, such as ethanol and acetonitrile. The solvophobic effect would drive the aryl substituent toward a configuration that minimizes its solvent exposed area.

An additional feature of a major conformational change in the excited state might involve transfer of electron density from the substituent to the highest-energy, semi-occupied molecular orbital. This latter situation would be favored by a geometry in which one of the aryl substituents lies coplanar with the Bodipy nucleus and would result in increased resonance stabilization of the excited state. Presumably, the barrier for such confor-

(36) (a) Molar volumes were calculated from energy-minimized structures for each substituent using SPARTAN.™ (b) SPARTAN, Wavefunction, Inc., Irvine, CA. (c) Hehre, W. J.; Shusterman, A. J.; Huang, W. W. *A Laboratory Book of Computational Organic Chemistry*; Wavefunction, Inc.: Irvine, CA. 1998.

(37) Li, F.; Yang, S. I.; Ciringh, Y.; Seth, J.; Martin, C. H.; III; Singh, D. L.; Kim, D.; Birge, R. R.; Bocian, D. F.; Holten, D.; Lindsey, J. S. *J. Am. Chem. Soc.* **1998**, *120*, 10001−10009.

(38) Englman, R.; Jortner, J. *Mol. Phys.* **1970**, *18*, 145−164.

(39) (a) Qin, W.; Baruah, M.; Van der Auweraer, M.; De Schryver, F. C.; Boens, N. *J. Phys. Chem. A* **2005**, *109*, 7371−7384. (b) Qin, W.; Baruah, M.; Stefan, A.; Van der Auweraer, M.; Boens, N. *ChemPhysChem* **2005**, *6*, 2343−2351.

(40) Figure 7 shows the computed structures for **3** but similar conclusions hold for the **5**, **6**, and **7**. Where comparison is possible, the computed ground-state geometries were in quite good agreement (bond lengths and angles around the B center) with the X-ray structures.

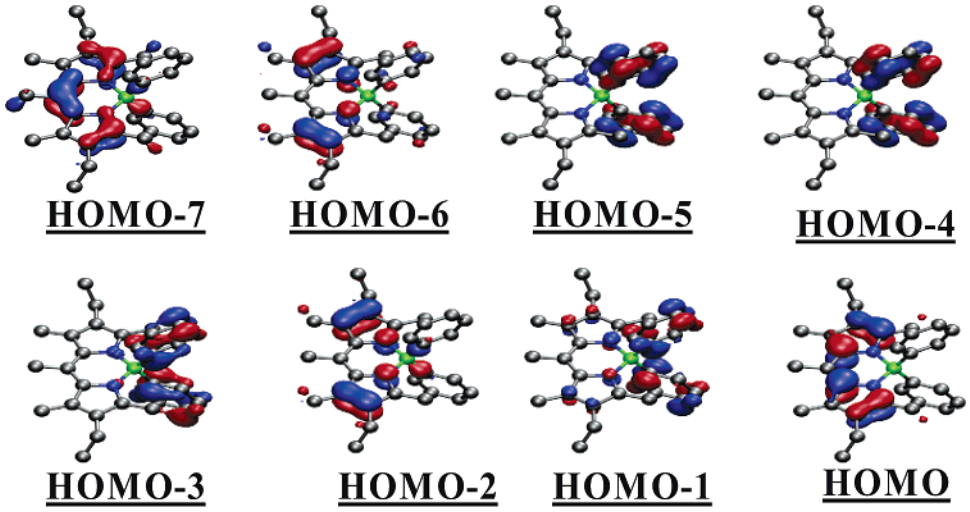

Figure 8. Computed highest-occupied molecular orbitals for the phenyl derivative **3**.

mational exchange is too high for the ground state but becomes possible by way of the increased potential energy available to the excited state. Preliminary computational studies have confirmed that the LUMO is localized on the Bodipy fragment in each case and that the first-allowed transition is from the Bodipy-localized HOMO to the LUMO. As the size of the aryl groups increases, there is an increased contribution to the S_1 state from lower-lying Bodipy-based orbitals. Furthermore, for **3**, the CI computational studies indicate the availability of occupied orbitals with considerable involvement of the phenyl rings (Figure 8). Mixing of these latter orbitals into the S_1 manifold might become more pronounced as the geometry is perturbed by solvent effects.

Concluding Remarks

A new class of Bodipy dyes has been prepared by replacing the fluorine substituents present in the more conventional chromophores with aryl substituents. Synthesis makes use of aryl-magnesium or aryl-lithium reagents. Using Grignard reagents, the monosubstituted derivatives are isolated but the use of lithium reagents leads to exclusive formation of the disubstituted derivatives. These synthetic protocols are generic and a wide range of substituted dyes is possible; the scope can be further extended by attaching chromophores to the meso position of the Bodipy unit. The optical and photophysical properties of the resultant B-aryl dyes depend on the size of the aryl group and on the nature of the surrounding solvent. The controlling feature appears to be a solvophobic effect in which the aryl substituent seeks to minimize surface contact with certain types of solvent. This geometry change might also involve buckling of the Bodipy framework. An interesting feature of the B-aryl dyes bearing pyrene substituents concerns the fact that intramolecular energy transfer from pyrene to Bodipy is quantitative. This effect serves to provide a series of additional excitation wavelengths that increase the virtual Stokes' shift; a highly desirable feature for flow cytometry and fluorescence microscopy.

Experimental Section

General methods are provide as Supporting Information.

4-Fluoro-4-phenyl-1,3,5,7,8-pentamethyl-2,4-diethyl-4-bora-3a, 4a-diaza-s-indacene (2). Bromobenzene (126 μL, 1.3 mmol) was added to a solution of magnesium (0.076 g, 3.1 mmol) in anhydrous diethyl ether (20 mL) maintained under argon. The mixture was stirred at room temperature for 1 h. The resulting solution was cooled to 0 °C and transferred via cannula to a solution of **1** (0.2 g, 0.63 mmol) in deoxygenated, freshly distilled diethyl ether (20 mL). The solution was stirred at 0 °C for 30 min, during which complete consumption of the starting material was observed by TLC. Water was added (5 mL), and the solution was extracted with CH_2Cl_2 (20 mL). After evaporation, the organic layer was purified by column chromatography on alumina (CH_2Cl_2/cyclohexane, 20:80), followed by recrystallization from CH_2Cl_2/hexane, yielding the desired compound (0.095 g, 40%).

^{1}H NMR ($CDCl_3$, 300 MHz): δ = 7.36−7.33 (m, 2H), 7.19−7.08 (m, 3H), 2.70 (s, 3H), 2.36 (s, 6H), 2.31 (q, 2H, ^3J = 7.7 Hz), 2.30 (q, 2H, ^3J = 7.7 Hz), 2.16 (s, 6H), 0.96 (t, 6H, ^3J = 7.7 Hz); ^{13}C {^{1}H} NMR ($CDCl_3$, 75 MHz): 151.9, 139.8, 134.95, 134.93, 132.4, 132.0, 131.9, 131.4, 126.9, 125.9, 31.0, 17.4, 17.2, 15.0, 14.6, 13.05, 13.00; ^{11}B {^{1}H} NMR ($CDCl_3$, 128 MHz): 5.73 (s); UV−vis (CH_2Cl_2) λ nm (ϵ, M^{-1} cm^{-1}) = 519 (175000), 370 (5200), 233 (17000); IR (KBr): ν = 3368 (m), 2961 (s), 1553 (s), 1447 (s), 1320 (s), 1190 (s), 978 (s), 762 (s); FAB$^+$ *m*/*z* (nature of peak, relative intensity): 377.2 ([M + H]$^+$, 100), 357.2 ([M−F]$^+$, 50); Anal. Calcd for $C_{24}H_{30}BFN_2$: C, 76.60; H, 8.04; N, 7.44. Found: C, 76.72; H, 8.25; N, 7.56.

4-Fluoro-4-(2-naphthyl)-1,3,5,7,8-pentamethyl-2,4-diethyl-4-bora-3a,4a-diaza-s-indacene (4). 2-Bromonaphthalene (52 mg, 0.25 mmol) was added to a solution of magnesium (6 mg, 0.25 mmol) in anhydrous THF (5 mL) maintained under argon. The mixture was stirred at room temperature for 1 h. The resulting solution was cooled to 0 °C and transferred via cannula to a degassed solution of **1** (80 mg, 0.25 mmol) in anhydrous THF (20 mL). The solution was stirred at 0 °C for 2 h, until complete consumption of the starting material was apparent by TLC. A solution of 3 M HCl in water was added (10 mL), and the solution was extracted with CH_2Cl_2 (20 mL). After evaporation, the organic layer was purified by column chromatography on silica (CH_2Cl_2/cyclohexane, gradient from 20:80 to 30:70), followed by recrystallization from CH_2Cl_2/hexane, to yield pure **4** (30 mg, 30%).

^{1}H NMR ($CDCl_3$, 300 MHz): δ = 7.97 (s, 1H), 7.81−7.72 (m, 2H), 7.62 (d, 1H, ^3J = 8.3 Hz), 7.39−7.26 (m, 3H), 2.75 (s, 3H), 2.39 (s, 6H), 2.29 (q, 4H, ^3J = 7.5 Hz), 2.17 (s, 6H), 0.94 (t, 6H, ^3J = 7.7 Hz); ^{13}C{^{1}H}NMR ($CDCl_3$, 75 MHz): 152.1, 139.9, 135.1, 133.1, 132.7, 132.5, 131.5, 131.1, 130.44, 130.38, 128.1, 127.6, 126.1, 125.0, 124.8, 17.4, 17.3, 15.0, 14.7, 13.2, 13.1; ^{11}B {^{1}H} NMR ($CDCl_3$, 128 MHz): 5.75 (s); UV−vis (CH_2Cl_2) λ nm (ϵ, M^{-1} cm^{-1}) = 516 (57000), 371 (5000), 230 (44500); IR (KBr): ν = 3047 (m), 2962 (s), 2928 (m), 2869 (m), 1554 (s), 1478 (s), 1403 (m), 1360 (m), 1320 (s), 1186 (s), 1110 (s), 977 (s), 915 (m), 819 (m), 716 (m); FAB$^+$ *m*/*z* (nature of

peak, relative intensity): 427.2 ([M + H]$^+$, 100); Anal. Calcd for $C_{28}H_{32}BFN_2$: C, 78.87; H, 7.56; N, 6.57. Found: C, 78.95; H, 7.82; N, 6.63.

4,4-Bis(2-naphthyl)-1,3,5,7,8-pentamethyl-2,4-diethyl-4-bora-3a,-4a-diaza-s-indacene (5). 2-Bromonaphthalene (104 mg, 0.5 mmol) was added to a solution of magnesium (12 mg, 0.5 mmol) in anhydrous THF (5 mL) maintained under argon. The mixture was stirred at room temperature for 1 h. The resulting solution, held at room temperature, was transferred via cannula to a degassed solution of **1** (80 mg, 0.25 mmol) in freshly distilled THF (20 mL). The solution was stirred for 2 h, until complete consumption of the starting material was observed by TLC. A solution of 3M HCl in water was added (10 mL), and the solution was extracted with CH_2Cl_2 (20 mL). After evaporation, the organic layer was purified by column chromatography on silica (CH_2Cl_2/cyclohexane, gradient from 20:80 to 30:70), followed by recrystallization from CH_2Cl_2/hexane, yielding pure **5** (53 mg, 30%).

^{1}H NMR ($CDCl_3$, 300 MHz): δ = 7.81−7.72 (m, 2H), 7.73−7.70 (m, 6H), 7.47 (dd, 2H, ^3J = 8.3 Hz, ^4J = 1.3 Hz), 7.41−7.38 (m, 4H), 2.72 (s, 3H), 2.42 (s, 6H), 2.36 (q, 4H, ^3J = 7.5 Hz), 1.73 (s, 6H), 0.99 (t, 6H, ^3J = 7.5 Hz); ^{13}C{^{1}H}NMR ($CDCl_3$, 75 MHz):152.8, 140.1, 133.7, 133.3, 132.7, 132.5, 132.4, 132.3, 132.1, 128.1, 127.4, 126.3, 124.8, 124.7, 18.0, 17.4, 15.0, 14.8; ^{11}B {^{1}H} NMR ($CDCl_3$, 128 MHz): 2.87 (s); UV−vis (CH_2Cl_2) λ nm (ϵ, M^{-1} cm^{-1}) = 516 (74500), 372 (10300), 234 (142000); IR (KBr): ν = 3360 (m), 3051 (m), 2958 (s), 2925 (s), 2854 (s), 1728 (s), 1631 (m), 1594 (m), 1557 (s), 1457 (s), 1262 (s), 1179 (m), 1119 (s), 1072 (m), 976 (m), 811 (m), 738 (m); FAB$^+$ *m*/*z* (nature of peak, relative intensity): 535.2 ([M + H]$^+$, 100); Anal. Calcd. for $C_{38}H_{39}BN_2$: C, 85.38; H, 7.35; N, 5.24. Found: C, 85.08; H, 7.52; N, 5.06.

General Procedure for the Preparation of Disubstituted C−Bodipy Compounds. In a Schlenk flask maintained at −78 °C, *n*-butyllithium (2.2 equiv) was added to a stirred, degassed solution of the relevant aryl bromide (2.2 equiv) in anhydrous THF or diethyl ether. The mixture was stirred at −78 °C for 1 h before warming to room temperature for a further 30 min. The resulting solution was transferred via cannula to a degassed solution of the precursor F-bodipy (1 equiv) in anhydrous THF (or diethyl ether). The solution was stirred at room temperature until complete consumption of the starting material was observed by TLC. Water was added, and the solution was extracted with CH_2Cl_2. After evaporation, the organic layer was purified by column chromatography and recrystallized from CH_2Cl_2/hexane.

4,4-Diphenyl-1,3,5,7,8-pentamethyl-2,4-diethyl-4-bora-3a, 4a-diaza-s-indacene (3). This compound was prepared according to the general procedure with bromobenzene (63 μL, 0.63 mmol) in 10 mL of diethyl ether, 0.51 mL of *n*-butyllithium (1.55 M in *n*-hexane) (formation of a pale yellow anion), and **1** (0.1 g, 0.31 mmol) in 20 mL of diethyl ether. Complete consumption of the starting material was observed after 30 min. Column chromatography was performed on alumina (CH_2Cl_2/cyclohexane, 20:80), and recrystallization gave 0.04 g of **3** (34%).

^{1}H NMR ($CDCl_3$, 400 MHz): δ = 7.24−7.11 (m, 10H), 2.67 (s, 3H), 2.37 (s, 6H), 2.33 (q, 4H, ^3J = 7.5 Hz), 1.7 (s, 6H), 0.96 (t, 6H, ^3J = 7.5 Hz); ^{13}C {^{1}H} NMR ($CDCl_3$, 100 MHz): 151.1, 139.9, 133.6, 133.4, 133.3, 132.3, 132.2, 127.1, 125.4, 17.9, 17.4, 15.2, 14.7, 14.6; ^{11}B {^{1}H} NMR ($CDCl_3$, 128 MHz): 2.70 (s); UV−vis (CH_2Cl_2) λ nm (ϵ, M^{-1} cm^{-1}) = 514 (64500), 376 (7800), 229 (28000); IR (KBr): ν = 3435 (m), 2961 (s), 1556 (s), 1451 (s), 1178 (s), 974 (s), 765 (s); FAB$^+$ *m*/*z* (nature of peak, relative intensity): 435.2 ([M + H]$^+$, 100), 357.2 ([M−C_6H_5]$^+$, 30); Anal. Calcd. for $C_{30}H_{35}BN_2$: C, 82.94; H, 8.12; N, 6.45. Found: C, 82.70; H, 7.87; N, 6.28.

4,4-Bis(4-methoxyphenyl)-1,3,5,7,8-pentamethyl-2,4-diethyl-4-bora-3a,4a-diaza-s-indacene (6). This compound was prepared according to the general procedure with 4-bromoanisole (79 μL, 0.63 mmol) in 10 mL of THF, 0.44 mL of *n*-butyllithium (1.55 M in *n*-hexane), and **1** (0.1 g, 0.31 mmol) in 20 mL of THF. Complete consumption of the starting material was observed after 5 min. Column chromatography was performed on alumina (CH_2Cl_2/cyclohexane, 20:80), and recrystallization gave 0.05 g of **6** (40% yield).

^{1}H NMR ($CDCl_3$, 300 MHz): δ = 6.94 (ABsys, 8H, J_{AB} = 8.6 Hz, $\nu_0\delta$ = 114.1 Hz), 3.77 (s, 6H), 2.67 (s, 3H), 2.36 (s, 6H), 2.33 (q, 4H, ^3J = 7.5 Hz), 1.72 (s, 6H), 0.98 (t, 6H, ^3J = 7.5 Hz); ^{13}C {^{1}H} NMR ($CDCl_3$, 75 MHz): 157.8, 151.3, 140.0, 134.8, 133.4, 132.4, 132.3, 112.7, 55.0, 18.1, 17.6, 15.2, 14.8, 14.7; ^{11}B {^{1}H} NMR ($CDCl_3$, 128 MHz): 2.56 (s); UV−vis (CH_2Cl_2) λ nm (ϵ, M^{-1} cm^{-1}) = 514 (93100), 380 (5400), 276 (28700), 233 (48000); IR (KBr): ν = 2960 (s), 1556 (s), 1176 (s), 974 (s), 819 (s); FAB$^+$ *m*/*z* (nature of peak, relative intensity): 495.2 ([M + H]$^+$, 100); Anal. Calcd. for $C_{32}H_{39}BN_2O_2$: C, 77.73; H, 7.95; N, 5.67. Found: C, 77.98; H, 8.04; N, 5.62.

4,4-Bis(1-pyrenyl)-1,3,5,7,8-pentamethyl-2,4-diethyl-4-bora-3a, 4a-diaza-s-indacene (7). This compound was prepared according to the general procedure with 1-bromopyrene (0.176 g, 0.63 mmol) in 10 mL of THF, 0.51 mL of *n*-butyllithium (1.55 M in *n*-hexane) (formation of a dark brown anion), and **1** (0.1 g, 0.31 mmol) in 20 mL of THF. Complete consumption of the starting material was observed after 30 min. Column chromatography was performed on alumina (CH_2Cl_2/cyclohexane, 20:80), and recrystallization gave 0.043 g of **7** (20%).

^{1}H NMR ($CDCl_3$, 400 MHz): δ = 8.25 (d, 2H, ^3J = 9.0 Hz), 8.12 (dd, 2H, ^3J = 8.0 Hz, ^4J = 1.5 Hz), 8.08 (dd, 2H, ^3J = 8.0 Hz, ^4J = 1.0 Hz), 8.01 (s, 4H), 7.94 (m, 4H), 7.79 (d, 2H, ^3J = 9.6 Hz), 7.38 (d, 2H, ^3J = 8.0 Hz), 2.48 (s, 3H), 2.32 (m, 10H), 1.38 (s, 6H), 0.96 (t, 3H, ^3J = 7.5 Hz), 0.91 (t, 3H, ^3J = 7.1 Hz); ^{13}C {^{1}H} NMR ($CDCl_3$, 100 MHz): 140.8, 135.7, 135.2, 133.1, 132.7, 131.8, 131.1, 130.4, 128.5, 127.9, 126.5, 125.6, 125.3, 124.9, 124.7, 124.16, 124.12, 18.6, 17.8, 15.4, 15.1, 14.8; ^{11}B {^{1}H} NMR ($CDCl_3$, 128 MHz): 4.97 (s); UV−vis (CH_2Cl_2) λ nm (ϵ, M^{-1} cm^{-1}) = 524 (46300), 351 (80000), 335 (50300), 279 (67000), 269 (43500), 247 (92000); IR (KBr): ν = 2960 (s), 1551 (s), 1432 (s), 1176 (s), 976 (s), 842 (s); FAB$^+$ *m*/*z* (nature of peak, relative intensity): 683.2 ([M + H]$^+$, 100), 481.1 ([M-pyrene]$^+$, 10); Anal. Calcd. for $C_{50}H_{43}BN_2$: C, 87.96; H, 6.35; N, 4.10. Found: C, 87.75; H, 6.17; N, 3.84.

Acknowledgment. This work was supported by EPSRC (EP/D001994/1), CNRS, Université Louis Pasteur de Strasbourg and the University of Newcastle. C.G. thanks IFET-ILO Contract 2001-33057 for financial support.

Supporting Information Available: General experimental procedure, reagents, materials physical methods, detailed X-ray crystal structure determination and geometrical parameters (Table S1) for compounds **4** and **6** (6 pages, print/PDF). This material is available free of charge via the Internet at http://pubs.acs.org.

JA062405A